Effectiveness of the statistical potential in the description of fermions in a worm-algorithm path-integral Monte Carlo simulation of ^{3}He atoms placed on a ^{4}He layer adsorbed on graphite

Humam B. Ghassib,[1] Asaad R. Sakhel,[2] Omar Obeidat,[2] Amer Al-Oqali,[3] and Roger R. Sakhel[4]

[1]*Department of Physics, The University of Jordan, Amman, Jordan*

[2]*Applied Sciences Department, Faculty of Engineering Technology, Al-Balqa Applied University, Amman 11134, Jordan*

[3]*Department of Physics, Mu'tah University, Al-Karak, Amman, Jordan*

[4]*Department of Basic Sciences, Faculty of Information Technology, Isra University, Amman 11622, Jordan*

(Received 20 September 2011; revised manuscript received 22 November 2011; published 4 January 2012)

We demonstrate the effectiveness of a statistical potential (SP) in the description of fermions in a worm-algorithm path-integral Monte Carlo simulation of a *few* ^{3}He atoms floating on a ^{4}He layer adsorbed on graphite. The SP in this work yields successful results, as manifested by the clusterization of ^{3}He, and by the observation that the ^{3}He atoms float on the surface of ^{4}He. We display the positions of the particles in 3D coordinate space, which reveal clusterization of the ^{3}He component. The correlation functions are also presented, which give further evidence for the clusterization.

DOI: 10.1103/PhysRevE.85.016702 PACS number(s): 02.70.−c, 67.60.Fp, 67.60.gf, 65.20.Jk

I. INTRODUCTION

The ^{3}He–He II sandwich system [1] and a system of ^{3}He atoms placed on ^{4}He layers are among the most fascinating He systems, thanks to their unusual properties. The investigation of this type of system on graphite is quite rare [2], and only a few similar studies along the same lines have been presented, for one component, either ^{3}He or ^{4}He, or their mixture [2–20]. An investigation involving ^{3}He atoms on a ^{4}He film adsorbed instead on Nuclepore [17,21] was also presented, as well as ^{3}He atoms on a superfluid ^{4}He film [14,17]. Several methods have been applied to explore the latter systems. For example, path-integral Monte Carlo (PIMC) has been applied for simulating helium films on a graphite surface [10,22], variational path-integral (VPI) Monte Carlo to investigate ^{4}He films adsorbed on alkali metal substrates [16], and diffusion Monte Carlo (DMC) to compute the ground-state properties of two-dimensional ^{4}He [8]. Further, variational Monte Carlo (VMC) was used to explore small mixed clusters of ^{3}He and ^{4}He atoms [23]. Nevertheless, because of the presence of the fermionic component, the simulation of systems containing ^{3}He using MC methods is not an easy task, although Ceperley [24] introduced earlier a PIMC method for the simulation of continuum fermions at nonzero temperature.

In this work, the worm-algorithm path-integral Monte Carlo (WAPIMC) method [25] is used to compute the thermal properties of a ^{3}He-^{4}He system where the ^{3}He floats on a ^{4}He film adsorbed on a graphite substrate. WAPIMC is a powerful technique, where one can simulate finite systems at finite temperatures in the grand canonical ensemble. That is, the exchange of particles with the surrounding particle reservoir is allowed. The number of particles is therefore allowed to change during a WAPIMC simulation and is controlled by the chemical potential. We are thus able to simulate a realistic situation, where particles can enter and leave the system. The latter feature is not found in other MC methods and is a big advantage for WAPIMC. In addition, WAPIMC enables us to investigate the microscopic properties, such as clusterization of helium atoms and the structural order. WAPIMC works also very well at high densities, and it can simulate a large number of particles $N \sim O(10^3)$. In contrast, the standard PIMC method [26] simulates systems only in the canonical ensemble at finite temperature and to $N \sim O(10^2)$. Whereas VPI and DMC work only at zero temperature, WAPIMC works at finite temperatures. One disadvantage of WAPIMC (and therefore PIMC) is that a simulation in the millikelvin temperature regime requires substantial computational time, of the order of a month, on a (for example) Intel Xeon workstation. Therefore WAPIMC simulations with T approaching zero would take years of CPU time.

In analytical approaches, previous work calculated the binding energy of ^{3}He-^{4}He [5] using an analytical variational procedure, following an ansatz due to Feynman (Ref. [6] in Gasparini *et al.* [5]); linear response theory was used to investigate the excitation spectrum of ^{3}He films adsorbed on substrates [27]; second order perturbation theory was applied to evaluate the ^{3}He-^{4}He effective interaction resulting from the exchange of third-sound quanta [6]; and Fermi-hypernetted-chain techniques were used to obtain the ground-state properties of a ^{3}He-^{4}He mixture using a wave function composed of a product of pair correlation functions [28]. A statistical-mechanical approach was further used to compute the thermodynamic properties of ^{3}He in thin ^{3}He-^{4}He films [29], and Krotscheck *et al.* [12] applied a variational theory with correlated basis functions to compute the phase diagram of ^{3}He-^{4}He mixtures in 2D. Although analytical methods are useful in obtaining macroscopic quantities like the thermodynamic properties (heat capacity, pressure, entropy, etc.), they lack the ability to display microscopic many-body features of the system, such as the structural properties, particle promotion and demotion between the layers, and the exchange of particles with a surrounding particle reservoir.

The interactions between helium atoms can usually be described by the HFDHE2 potential of Aziz *et al.* [30]. However, in the systems considered here, the ^{3}He component is initially quite dilute as we begin the simulation with a small number of ^{3}He atoms. The ^{3}He component can therefore be approximated by an ideal gas. Such an ideal system can in turn be described by a Slater determinant composed of noninteracting single-particle wave functions, and consequently the

exchange of two fermions leads to a change in the sign of the total wave function. In the case of an interacting system, the wave function is a many-body wave function combined of a product of single-particle wave functions and a train of Jastrow functions $\prod_{i<j} f(r_{ij})$. The Jastrow function $f(r_{ij})$, where r_{ij} is the distance between atoms i and j, describes the interactions between the particles in the wave function. Therefore, the Slater determinant includes correlations between the particles, and no sign change arises when two fermions are swapped. Although in the current simulations we do not use a Slater determinant, the presence of fermions causes the well-known sign problem [31] to arise when two fermions are swapped in a dilute system. Our purpose in this work is to present a method to circumvent the sign problem in a worm-algorithm path-integral Monte Carlo (WAPIMC) [25] simulation of a ^{3}He-^{4}He system, where the MC statistics blow up to infinity if the partition function goes to zero [32]. We propose to disallow the swap of fermions and to use instead a so-called statistical potential (SP) [33]. The SP describes "statistical interactions" between fermions. Earlier, Anderson and Miller [6] included the effects of a hard core in the ^{3}He-^{3}He interaction potential to describe their repulsion.

In this paper, our chief goal is to demonstrate the effectiveness of the SP in a WAPIMC simulation of a *few* ^{3}He atoms placed on a layered ^{4}He structure adsorbed on graphite. We focus mainly on the clusterization of the ^{3}He component [2,34,35] driven by an effective interaction, resulting from a combination of interaction potentials in the system. We therefore present figures displaying the positions of the particles, which reveal the clusterization of the ^{3}He component. The correlations between the helium atoms are also explored, which provide further evidence for clusterization. This paper reports a sample of results from the current project of a few ^{3}He atoms on a ^{4}He layer adsorbed on graphite. This project is part of a set of investigations involving a previous examination of the ^{3}He-^{4}He sandwich system [36] and a future one of ^{4}He in Vycor.

Our key results are as follows. First, the SP is effective in describing the fermions in a WAPIMC simulation because (i) it allows the ^{3}He atoms to "float" on the outer surface of ^{4}He in agreement with experimental observations [2,14]; (ii) it does not prohibit the clusterization of ^{3}He atoms which display strong correlations; and (iii) the energies of the ^{3}He atoms are in line with values reported earlier [5]. Second, the properties of the system are found to be largely sensitive to the chemical potential, particularly the final number of ^{3}He atoms that can be achieved at the end of a simulation. However, it was found that the error bars of the WAPIMC simulation are somewhat large at temperatures $T < 80$ mK, whereas at $T \geqslant 80$ mK they are small. Further, we would like to draw attention to the fact that, in the temperature range considered, it was very hard to obtain a number of ^{3}He atoms of the order $\sim O(1)$. The simulation always ended up with $\sim O(10)$.

II. METHOD

In what follows, we briefly outline the method. We modified a previously written WAPIMC code [25,32], originally developed for the ^{4}He on graphite (used in Ref. [19]) to include the ^{3}He component, as explained in our previous paper [36]. However, the positioning of the ^{3}He atoms is slightly different from the sandwich structure [36], as we place the ^{3}He atoms only on the outer surface of the ^{4}He layer. In addition, we did not apply the mass-update procedure of a fictitious particle as in Refs. [36,37]. This is because the ^{3}He atoms floating on the surface of ^{4}He already have a high mobility. The ^{3}He-^{4}He as well as the ^{4}He-^{4}He interactions are, as usual, described by the HFDHE2 potential of Aziz *et al.* [30]. On the other hand, the ^{3}He component is dilute and can therefore be considered an ideal gas. However, there are important ^{3}He interactions which are statistical in nature. That is, the fermionic nature of ^{3}He enters into play through the SP [33]:

$$v_{\mathrm{SP}}(r) = -k_B T \ln\left[1 - \exp\left(-2\pi r^2/\lambda_{dB}^2\right)\right], \qquad (1)$$

r being the distance between a pair of particles, and λ_{dB} the thermal de Broglie wavelength. Yet, the code is very much the same as in Ref. [36]. The simulations were conducted in the grand canonical ensemble (GCE) in the millikelvin temperature regime, with carefully chosen chemical potentials for which the number of ^{3}He atoms would not "disappear" later into the surrounding particle reservoir. It was difficult to find chemical potentials for which the simulations would simultaneously evolve effectively and stabilize at a reasonable number of ^{3}He atoms. We found that it was very difficult to stabilize the number of ^{3}He atoms to $O(\sim 1)$.

The dimensions of the simulation box were fixed at $19.693 \times 17.054 \times 26.798$ Å^3 for all systems, set by a predefined density. Each simulation was initialized with a few (from 2 to 15) ^{3}He atoms placed on the surface of 72 ^{4}He atoms comprising two layers, adsorbed on the surface of a graphite substrate. For 2–15 ^{3}He atoms, the ^{3}He coverage lies between 0.5 and 4 % and is quite dilute (cf. Ref. [12]). Then it was run for several weeks of CPU time until thermalization stabilized the energy within a certain error bar. The time step chosen was $\tau = (1/400)$ K^{-1}, and the temperatures and chemical potentials used are tabulated in Tables I and II. The values of μ listed are renormalizated values, by the self-energy of the interacting particles Σ, i.e., $\mu = \mu_0 + \Sigma$, where μ_0 is an initial chemical potential of our choice.

In this work we essentially let the chemical potential decide the number of particles in our system by running it in the GCE. Consequently, the numbers of ^{3}He and ^{4}He particles, $\langle N_3 \rangle$ and $\langle N_4 \rangle$ respectively, are updated from their initial values depending on the magnitude of the chemical potential. In passing, it is interesting to note that the gradual dynamic update of $\langle N_3 \rangle$ during thermal evolution represents the well-known adiabatic switching-on process of the ^{3}He interaction [38]. Interestingly enough, this might be an experimental analog to the Gell-Mann-Low theorem [39].

III. RESULTS AND DISCUSSION

A. Structural properties

We begin with a visualization of the spatial positions of the ^{3}He and ^{4}He atoms for two of our systems in 3D coordinates, so as to check for clusterization of the ^{3}He component. Figures 1 and 2 display these positions for systems at $T = 60$, 70, and 100 mK with $\mu = -14.392$, -14.139, and -11.216 K, respectively. More details about these systems are found in

TABLE I. WAPIMC thermal properties of a system of a number of ^{3}He atoms placed on a ^{4}He layer adsorbed on a graphite substrate at temperatures ranging from $T = 60$ to 100 mK, labeled a–e, respectively. From left to right: System label, temperature T in mK, chemical potential μ, average total number of particles $\langle N\rangle$, total energy per particle $\langle E\rangle/\langle N\rangle$, pressure per particle $\langle P\rangle/\langle N\rangle$, entropy per particle $\langle S\rangle/\langle N\rangle$ (unitless), internal energy per particle $\langle U\rangle/\langle N\rangle$, and superfluid fraction ρ_s/ρ. Each thermal property indicated is a thermodynamic average in units of K, except for the entropy which is unitless.

System	T (mK)	μ (K)	$\langle N\rangle$	$\langle E\rangle/\langle N\rangle$ (K)	$\langle P\rangle/\langle N\rangle$ (K)	$\langle S\rangle/\langle N\rangle$	$\langle U\rangle/\langle N\rangle$ (K)	ρ_s/ρ (%)
a	60	−14.392	127.24	−47.988	5.507×10^{-2}	2473.57	−74.662	1.936
			±7.48	±4.425	$\pm 3.261 \times 10^{-3}$		±3.071	±0.398
b	70	−14.139	125.55	−53.027	5.489×10^{-2}	2304.26	−78.679	1.755
			±7.07	±4.948	$\pm 1.609 \times 10^{-2}$		±1.886	±0.544
c	80	−15.397	91.987	−56.575	8.129×10^{-2}	1959.80	−92.741	8.426
			$\pm 2.632 \times 10^{-3}$	±0.681	$\pm 9.338 \times 10^{-3}$		±0.450	±0.217
d	90	−9.003	162.27	−44.249	3.775×10^{-2}	1398.28	−64.348	3.051
			±0.906	±0.296	$\pm 2.450 \times 10^{-4}$		±0.157	$\pm 2.929 \times 10^{-2}$
e	100	−11.216	133.25	−45.294	5.710×10^{-2}	1463.56	−70.411	0.210
			±0.614	±0.809	$\pm 1.696 \times 10^{-3}$		±0.491	±0.105

Tables I and II, which we shall elaborate below. The ^{3}He atoms are the solid green circles, whereas the ^{4}He atoms are the solid red triangles. The vertical positions (z) are with respect to the graphite surface in the xy plane. One can see that there are two ^{4}He layers, above which a ^{3}He component resides. In Figs. 1 and 2, a partial clusterization of ^{3}He is observed. The clusterization of the ^{3}He atoms in a ^{4}He environment was predicted earlier by Ghassib and Chatterjee [34], as well as by Ghassib [35]. Nanoclusterization of the ^{3}He fluid in the same system as ours was observed earlier [2]. In addition, Krotscheck *et al.* [12] found that the effective interaction between ^{3}He impurities in ^{4}He is sufficiently attractive to generate ^{3}He dimers. One could argue that ^{3}He clusterization is rather surprising, since the interactions between the ^{3}He atoms are repulsive, as dictated by the fermionic SP, and because the ^{3}He atoms have a large zero-point motion. Further, the ^{3}He atoms at $z \sim 9$ Å in Figs. 1 and 2 are located at positions where they only feel the weak tail of the graphite potential (Ref. [25] in Corboz *et al.* [19]), and hence this effect can largely be excluded for ^{3}He. In contrast, the ^{3}He atoms strongly feel the ^{3}He-^{4}He interaction at a vertical distance of ∼3 Å from the second ^{4}He layer. Therefore at low T, ^{3}He-^{4}He mixing overcomes the repulsive statistics of the ^{3}He atoms and does not allow them to aggregate into a separate phase. The ^{3}He-^{4}He interaction further localizes the ^{3}He atoms on the ^{4}He surface [14,21,40], as it enhances the effective mass of ^{3}He atoms [3,14,17]. The increase in the effective mass therefore overcomes the effects of the large zero-point motion of the ^{3}He atoms. Some ^{4}He atoms have been promoted (i.e., "evaporated") to the ^{3}He layers in the course of the thermalization process. This is an inevitable consequence of any vacancies introduced into the ^{3}He cloud. As the temperature is increased, clusterization of ^{3}He ceases to exist as displayed in Fig. 3 at 100 mK. This is because as one increases T, the repulsive statistics becomes stronger in Eq. (1) and begins to overcome the ^{3}He-^{4}He mixing effects. One can then argue that the SP can account for a larger solubility of ^{3}He into the ^{4}He at low T. One further observes that the ^{3}He component has separated into a floating phase above the ^{4}He component, which is also driven by a larger ^{3}He density. Not one single ^{3}He atom has evaporated into the ^{3}He phase.

It must be mentioned that the finiteness of the system and the boundary conditions play a decisive role in the clusterization process of the ^{3}He atoms. As the system becomes more confined, the ^{3}He atoms approach the ^{4}He atoms which increases the binding, and therefore ^{3}He clusterization is enhanced. Next to this, the box-wall boundaries of our simulation cell cause the matter waves of the ^{3}He atoms to

TABLE II. As in Table I, except for the ^{3}He component of the same systems with the kinetic energy per particle at the end instead of the superfluid fraction.

System	T (mK)	μ (K)	$\langle N_3\rangle$	$\langle E_3\rangle/\langle N\rangle$ (K)	$\langle P_3\rangle/\langle N\rangle$ (K)	$\langle S_3\rangle/\langle N\rangle$	$\langle U_3\rangle/\langle N\rangle$ (K)	$\langle K_3\rangle/\langle N\rangle$
a	60	−14.392	40.576	−2.095	4.326×10^{-5}	165.37	−4.633	3.595
			±5.421	±1.108	$\pm 8.347 \times 10^{-3}$		±0.534	±0.455
b	70	−14.139	34.308	−1.717	1.674×10^{-4}	150.91	−4.263	3.394
			±5.766	±1.224	$\pm 5.463 \times 10^{-3}$		±0.638	±0.447
c	80	−15.397	12.412	−0.888	1.055×10^{-2}	539.01	−2.648	2.251
			$\pm 6.908 \times 10^{-2}$	$\pm 4.923 \times 10^{-3}$	$\pm 7.803 \times 10^{-6}$		$\pm 3.677 \times 10^{-3}$	$\pm 1.180 \times 10^{-3}$
d	90	−9.003	76.961	−1.874	2.031×10^{-2}	1122.80	−5.451	4.626
			±0.881	±0.083	$\pm 1.312 \times 10^{-4}$		$\pm 6.661 \times 10^{-2}$	$\pm 5.769 \times 10^{-3}$
e	100	−11.216	60.698	−2.344	2.753×10^{-2}	1056.12	−4.713	3.634
			±0.338	±0.139	$\pm 7.230 \times 10^{-5}$		$\pm 6.280 \times 10^{-2}$	$\pm 6.031 \times 10^{-2}$

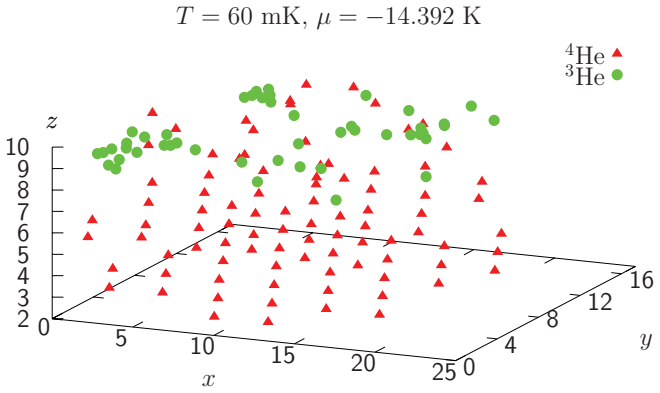

FIG. 1. (Color online) WAPIMC spatial positions of the atoms for a system of ^{3}He placed on the surface of a ^{4}He layer adsorbed on a graphite substrate at $T = 60$ mK. The total number of particles is $\langle N\rangle = 127.24 \pm 7.48$ and the number of ^{3}He atoms is $\langle N_3\rangle = 40.576 \pm 5.421$. The chemical potential is fixed at $\mu = -14.392$ K. Solid red triangles, ^{4}He atoms; solid green circles, ^{3}He atoms. x, y, and z are in units of Å.

be reflected from the hard walls, and therefore may result in standing matter waves inside the ^{3}He-^{4}He system.

Importantly, the number of bosons alone plays also an important role in the clusterization of the fermions. According to Guardiola and Navarro [23], the clusterization of ^{3}He atoms in an environment of ^{4}He atoms requires a certain number of bosons, N_B, in order to overcome the effects of zero-point motion and fermionic repulsion. It was expected [23] that a small number of bosons N_B and a large number of fermions N_F will cause instabilities in the mixture. Further, for only one ^{4}He atom a ^{3}He cluster could only be achieved if N_F was above 20. Next to this, bound states of ^{3}He-^{4}He were anticipated for $20 < N_F < 30$. Peculiarly, the above authors found that two ^{4}He atoms cannot achieve a ^{3}He cluster if $3 < N_F < 17$.

B. Adequacy of statistical potential

Evidently, the SP used to describe the fermions seems to be effective, as dictated by the results in Sec. III A, particularly because it allows the ^{3}He atoms to float on the ^{4}He surface. The ^{3}He pair distances in Figs. 1–3 are $r \sim O(1$ Å) and therefore much smaller than the de Broglie wavelength λ_{dB} for ^{3}He

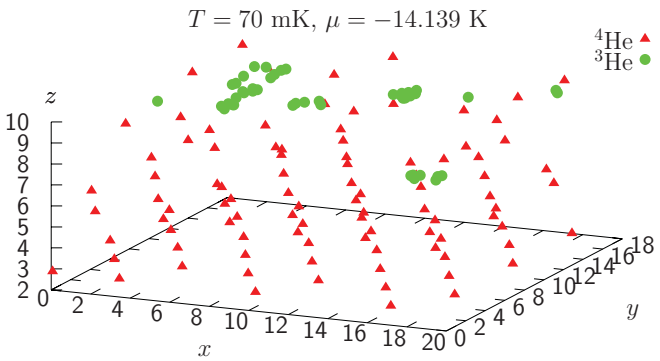

FIG. 2. (Color online) As in Fig. 1, but for $T = 70$ mK with $\mu = -14.139$ K, $\langle N\rangle = 125.55 \pm 7.07$, and $\langle N_3\rangle = 34.308 \pm 5.766$. x, y, and z are in units of Å.

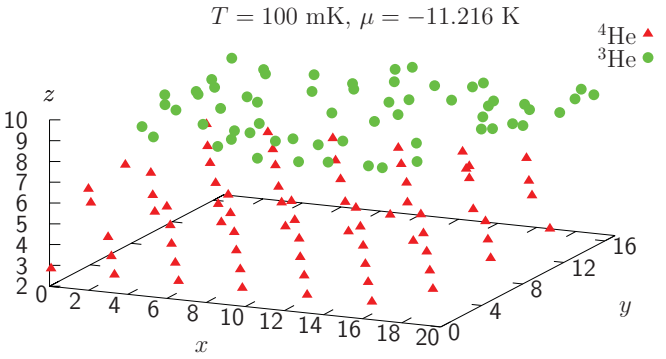

FIG. 3. (Color online) As in Fig. 1, but for $T = 100$ mK with $\mu = -11.216$ K, $\langle N\rangle = 133.25 \pm 0.614$, and $\langle N_3\rangle = 60.698 \pm 0.338$. x, y, and z are in units of Å.

atoms, where λ_{dB} lies between 41.51 Å at $T = 60$ mK and 31.87 Å at $T = 100$ mK. The Fermi-Dirac statistical potential (1) goes to zero as r/λ_{dB} becomes larger than 1, and in our case $r/\lambda_{dB} \ll 1$ for ^{3}He pairs. Thus the SP is adequate for the description of the ^{3}He atoms in our systems. Further, the "range" of the SP in the above temperature range is significant, approximately equal to λ_{dB} for the latter temperatures. As the temperature is increased, the range of the SP decreases, and its repulsion becomes stronger. Essentially, then, spatial pair correlations between the ^{3}He atoms are significant.

C. Thermal properties

Next, we present some numerical WAPIMC results for the thermal properties of this type of system. As such, Table I displays results for the whole system, i.e., ^{3}He and ^{4}He together on graphite. From left to right the table lists a system label, the temperature T in mK, renormalized chemical potential μ, total number of particles $\langle N\rangle$, total energy per particle $\langle E\rangle/\langle N\rangle$, pressure per particle $\langle P\rangle/\langle N\rangle$, entropy per particle $\langle S\rangle/\langle N\rangle$ (unitless), internal energy per particle $\langle U\rangle/\langle N\rangle$, and superfluid fraction ρ_s/ρ (which is for ^{4}He only). The superfluid fraction was computed using the winding number approach according to formula (3.31) in the excellent review of Ceperley [26]:

$$\frac{\rho_s}{\rho} = \frac{\langle \mathbf{W}^2\rangle}{2\lambda\beta N}, \tag{2}$$

ρ_s and ρ being the superfluid and total density, respectively, $\lambda = \hbar^2/(2m)$, $\beta = M\tau$, and N the number of particles. $\mathbf{W}$ is the winding number given by

$$\mathbf{W} = \sum_{i=1}^{N}\sum_{j=1}^{M}(\mathbf{r}_{i,j-1} - \mathbf{r}_{i,j}), \tag{3}$$

where $\mathbf{r}_{i,j}$ is the position of the ith particle at the jth time slice. In essence, we exclude the ^{3}He atoms in the evaluation of $\mathbf{W}$. Thus, the superfluid density would correspond to the fraction of ^{4}He atoms which are able to flow without friction in the higher layers away from the graphite surface. The ^{4}He layers close to the graphite surface are in the solid phase at low temperatures. Each thermal property $\langle\cdots\rangle$ indicated is the WAPIMC thermodynamic average in units of K, except for the entropy and number of particles which are unitless. Table II is the same as Table I, except that it displays the ^{3}He statistics

separately, indicated by a subscript "3" in each thermal property, with the kinetic energy per particle $\langle K_3\rangle/\langle N\rangle$ in the last column instead of ρ_s/ρ. We emphasize that the properties in Table II include essentially the effects of the ^{4}He as well as the graphite potential environment. There are five systems at temperatures ranging from $T = 60$ to 100 mK, labeled from a to e, respectively. For 60 and 70 mK, the same systems of Figs. 1 and 2 are considered, labeled a and b, respectively. The energies $\langle E\rangle/\langle N\rangle$ of the systems are negative, signaling that they have reached stable configurations. The energy of the ^{3}He component $\langle E_3\rangle/\langle N\rangle$ (for systems a–e) is also negative, revealing that it may have formed bound states with the ^{4}He [5]. Further, our ^{3}He energies are in line with those obtained by Gasparini *et al.* [5] for ^{3}He on a ^{4}He film of 13 Å thickness. Being far away from the graphite surface, our ^{3}He atoms have a much smaller energy per particle $|\langle E_3\rangle/\langle N\rangle|$ than the ^{4}He component $(|\langle E\rangle - \langle E_3\rangle|/\langle N\rangle)$. The ^{3}He energy has a large kinetic component $\langle K_3\rangle/\langle N\rangle$, or quantum pressure, as compared to its internal energy $\langle U_3\rangle/\langle N\rangle$, but it is small compared to the total energy of the system. By going to higher temperatures, such as $T \geqslant 80$ mK, $\langle S_3\rangle/\langle N\rangle$ rises substantially as compared to $\langle S\rangle/\langle N\rangle$. For example, it may be easily verified that $\langle S_3\rangle/\langle S\rangle$ is ∼80 and 70% for d and e ($T > 80$ mK), respectively, whereas it is less than 10% for a and b ($T < 80$ mK). Therefore, there is a lower order associated with ^{3}He at $T > 80$ mK. The small values of ρ_s/ρ reveal that the ^{3}He atoms deplete the superfluid substantially. The pressure in Table I remains of order 10^{-2} K for all systems, and is largest for system c which has the largest chemical potential $|\mu|$. In Table II it is of orders 10^{-5} and 10^{-4} K for a and b, respectively, and for c–e it is order 10^{-2} K. However, for a and b the error bar is very large. An interesting WAPIMC calculation to pursue in the future would be for a system of ^{3}He atoms placed on a ^{4}He surface without a graphite substrate.

From the tables, one can compute the same quantities separately for ^{4}He and ^{3}He, such as the energy of ^{4}He per ^{4}He particle, $\langle E_4\rangle/\langle N_4\rangle$, or ^{3}He per ^{3}He particle, $\langle E_3\rangle/\langle N_3\rangle$. The values have been listed in the tables found in the Supplementary Material [41]. However, the error bars need to be carefully computed using common rules for the different mathematical operations on these error bars. Typical values obtained are $\langle E_4\rangle/\langle N_4\rangle = (-67.381 \pm 10.589)$ K and $\langle E_3\rangle/\langle N_3\rangle = (-6.570 \pm 3.605)$ K at $T = 60$ mK. Particularly, the binding energy of ^{3}He, $\langle U_3\rangle/\langle N_3\rangle$, is $\sim O(-10)$ K.

D. Pair correlations

The pair correlation function $g(r)$ provides further information about the structure of the systems, where r is the distance between a pair of particles. Figure 4 displays $g(r)$ for the systems a (red crosses), b (open green squares), and d (solid blue squares) listed in Table I. For each temperature, one observes four peaks: a major one at $r \sim 1$ Å, and consecutively at ∼3, ∼5.9, and ∼8.5 Å, respectively. By referring to the structure in Figs. 1 and 2, one can understand that the first peak in Fig. 4 is for the clusterized ^{3}He atoms, since these display the smallest interparticle distances. The rest of the peaks are largely associated with the correlations between the ^{4}He atoms in the layers $z \sim 3$ Å and $z \sim 6$ Å. That is, the peak at $r \sim 3$ Å is for ^{4}He particles surrounded by their

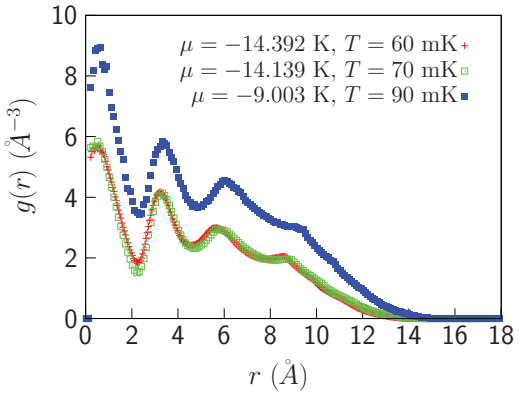

FIG. 4. (Color online) Correlation function $g(r)$ for systems a (red crosses), b (open green squares), and d (solid blue squares) listed in Table I.

first nearest neighbors, the one at $r \sim 5.9$ Å for ^{4}He atoms and their second nearest neighbors, etc. At 90 mK, the correlations are stronger than at the other temperatures, because system d has the largest number of helium atoms among the systems displayed in the tables. The $g(r)$ for $T = 60$ and 70 mK are almost identical with little differences.

IV. CONCLUSION

In summary, we have demonstrated the effectiveness of a repulsive statistical potential (SP) in the description of fermions in a WAPIMC simulation of a few ^{3}He atoms floating on a ^{4}He layer adsorbed on a graphite substrate. The use of this SP yields results in agreement with earlier experimental observations, where the ^{3}He component preferentially floats on the outer surface of the ^{4}He layer [2,14], and occupies surface states [6]. Further, the SP allows the clusterization of the ^{3}He component [2,34,35]. As one increases the temperature, the clusterization of ^{3}He ceases to exist as the ^{3}He-^{4}He statistical repulsion becomes stronger, thereby overcoming ^{3}He-^{4}He mixing. Eventually, the ^{3}He component separates into a floating phase above the ^{4}He surface. We additionally computed some thermal properties of these systems in the millikelvin temperature regime. The total energies of these systems turned out to be negative, indicating that these systems have reached their thermal equilibrium. The quantum pressure of the ^{3}He component turns out to be ∼10% of the total energy, and the disorder in ^{3}He rises sharply beyond $T = 80$ mK. The superfluid component in ^{4}He is substantially depleted as a result of adding ^{3}He. Finally, our ^{3}He energies are in line with those reported earlier by Gasparini *et al.* [5].

ACKNOWLEDGMENTS

The authors acknowledge financial support from The University of Jordan. One of us (H.B.G.) is grateful to The University of Jordan for granting him a sabbatical leave during which the present work was undertaken under the general title "Many-Body Systems: Further Studies and Calculations [Part Two]." The authors also thank Nikolay Prokof'ev for providing them with his WAPIMC code and for his great help in its modification.

[1] Humam B. Ghassib and Yahya F. Waqqad, Physica B **194–196**, 511 (1994).
[2] F. Ziouzia, J. Nyéki, B. Cowan, and J. Saunders, Physica B **329–333**, 252 (2003).
[3] Michael J. Di Pirro and Francis M. Gasparini, Phys. Rev. Lett. **44**, 269 (1980).
[4] D. McQueeney, G. Agnolet, and J. D. Reppy, Phys. Rev. Lett. **52**, 1325 (1984).
[5] Francis M. Gasparini, Bidyut Bhattacharyya, and Michael J. DiPirro, Phys. Rev. B **29**, 4921 (1984).
[6] R. H. Anderson and M. D. Miller, Phys. Rev. B **40**, 2109 (1989).
[7] H. Alles, J. P. Ruutu, A. V. Babkin, and P. J. Hakonen, Phys. Rev. Lett. **73**, 1388 (1994).
[8] S. Giorgini, J. Boronat, and J. Casulleras, Phys. Rev. B **54**, 6099 (1996).
[9] M. Dann, J. Nyeki, B. Cowan, and J. Saunders, J. Low. Temp. Phys. **110**, 627 (1998).
[10] Marlon Pierce and Efstratios Manousakis, Phys. Rev. B **63**, 144524 (2001).
[11] R. H. Anderson and M. D. Miller, Cond. Matt. Phys. **4**, 335 (2001).
[12] E. Krotscheck, J. Paaso, M. Saarela, and K. Schörkhuber, Phys. Rev. B **64**, 054504 (2001).
[13] R. H. Anderson and M. D. Miller, Phys. Rev. B **66**, 174511 (2002).
[14] R. B. Hallock, Physica B **329–333**, 154 (2003).
[15] H. Akimoto and R. B. Hallock, Physica B **329–333**, 164 (2003).
[16] Massimo Boninsegni and Leszek Szybisz, Phys. Rev. B **70**, 024512 (2004).
[17] H. Akimoto, J. D. Cummings, and R. B. Hallock, Phys. Rev. B **73**, 012507 (2006).
[18] M. Neumann, J. Nyéki, Brian Cowan, and John Saunders, Science **317**, 1356 (2007).
[19] Phillippe Corboz, Massimo Boninsegni, Lode Pollet, and Matthias Troyer, Phys. Rev. B **78**, 245414 (2008).
[20] M. C. Gordillo and J. Boronat, Phys. Rev. Lett. **102**, 085303 (2009).
[21] P. A. Sheldon and R. B. Hallock, Phys. Rev. Lett. **77**, 2973 (1996).
[22] M. Pierce and E. Manousakis, Phys. Rev. B **59**, 3802 (1999).
[23] R. Guardiola and J. Navarro, Phys. Rev. Lett. **89**, 193401 (2002).
[24] D. M. Ceperley, Phys. Rev. Lett. **69**, 331 (1992).
[25] M. Boninsegni, N. V. Prokof'ev, and B. V. Svistunov, Phys. Rev. E **74**, 036701 (2006).
[26] D. M. Ceperley, Rev. Mod. Phys. **67**, 279 (1995).
[27] M. M. Calbi and E. S. Hernãndez, J. Low. Temp. Phys. **120**, 1 (2000).
[28] A. Fabrocini and A. Polls, Phys. Rev. B **25**, 4533 (1982).
[29] R. H. Anderson and M. D. Miller, Phys. Rev. B **66**, 174511 (2002).
[30] R. A. Aziz, V. P. S. Nain, J. S. Carley, W. L. Taylor, and G. T. McConville, J. Chem. Phys. **70**, 4330 (1979).
[31] Matthias Troyer and Uwe-Jens Wiese, Phys. Rev. Lett. **94**, 170201 (2005).
[32] N. V. Prokof'ev (private communication). Nikolay Prokof'ev provided us with his worm-algorithm code. He also helped us in its modification to include a ^{3}He component.
[33] R. K. Pathria, *Statistical Mechanics*, 2nd ed. (Butterworth Heinemann, Oxford, 2004).
[34] H. B. Ghassib and S. Chatterjee, in *Proceedings of the 17th International Conference on Low Temperature Physics (LT 7)*, Part II—Contributed Papers, Universitaet Karlsruhe and Kernforschungszentrum Karlsruhe, edited by U. Eckern *et al.* (North-Holland, Amsterdam, 1984), p. 1241.
[35] H. B. Ghassib, Z. Phys. B **56**, 91 (1984).
[36] Amer Al-Oqali, Asaad R. Sakhel, and Humam B. Ghassib, e-print arXiv:cond-mat/1105.5714.
[37] P. Corboz, L. Pollet, N. V. Prokof'ev, and M. Troyer, Phys. Rev. Lett. **101**, 155302 (2008).
[38] David Pines and Phillipe Noziéres, *The Theory of Quantum Liquids* (Perseus Books Publishing, LLC, Cambridge, MA, 1999).
[39] Murray Gell-Mann and Francis Low, Phys. Rev. **84**, 350 (1951).
[40] D. T. Sprague, N. Alikacem, and R. B. Hallock, Phys. Rev. Lett. **74**, 4479 (1995).
[41] See Supplemental Material at http://link.aps.org/supplemental/10.1103/PhysRevE.85.016702.